

Multiplicity dependent J/ψ and $\psi(2S)$ production at forward and backward rapidity in $p+p$ collisions at $\sqrt{s} = 200$ GeV

N.J. Abdulameer,^{14,21} U. Acharya,¹⁸ C. Aidala,⁴⁰ Y. Akiba,^{53,54,*} M. Alfred,²⁰ V. Andrieux,⁴⁰ S. Antsupov,⁵⁶ N. Apadula,²⁶ H. Asano,^{32,53} B. Azmoun,⁷ V. Babintsev,²² N.S. Bandara,³⁸ E. Bannikov,⁵⁶ K.N. Barish,⁸ S. Bathe,^{5,54} A. Bazilevsky,⁷ M. Beaumier,⁸ R. Belmont,^{11,47} A. Berdnikov,⁵⁶ Y. Berdnikov,⁵⁶ L. Bichon,⁶⁴ B. Blankenship,⁶⁴ D.S. Blau,^{31,44} J.S. Bok,⁴⁶ V. Borisov,⁵⁶ M.L. Brooks,³⁴ J. Bryslawskij,^{5,8} V. Bumazhnov,²² S. Campbell,¹² R. Cervantes,⁵⁹ D. Chen,⁵⁹ M. Chiu,⁷ C.Y. Chi,¹² I.J. Choi,²³ J.B. Choi,^{28,†} Z. Citron,⁶⁵ M. Connors,^{18,54} R. Corliss,⁵⁹ N. Cronin,⁵⁹ M. Csanád,¹⁵ T. Csörgő,^{39,66} T.W. Danley,⁴⁸ M.S. Daugherty,¹ G. David,^{7,59} K. DeBlasio,⁴⁵ K. Dehmelt,⁵⁹ A. Denisov,²² A. Deshpande,^{54,59} E.J. Desmond,⁷ A. Dion,⁵⁹ D. Dixit,⁵⁹ V. Doomra,⁵⁹ J.H. Do,⁶⁷ A. Drees,⁵⁹ K.A. Drees,⁶ J.M. Durham,³⁴ A. Durum,²² H. En'yo,⁵³ A. Enokizono,^{53,55} R. Esha,⁵⁹ B. Fadem,⁴² W. Fan,⁵⁹ N. Feege,⁵⁹ D.E. Fields,⁴⁵ M. Finger, Jr.,⁹ M. Finger,⁹ D. Firak,^{14,59} D. Fitzgerald,⁴⁰ S.L. Fokin,³¹ J.E. Frantz,⁴⁸ A. Franz,⁷ A.D. Frawley,¹⁷ Y. Fukuda,⁶² P. Gallus,¹³ C. Gal,⁵⁹ P. Garg,^{3,59} H. Ge,⁵⁹ F. Giordano,²³ Y. Goto,^{53,54} N. Grau,² S.V. Greene,⁶⁴ M. Grosse Perdekamp,²³ T. Gunji,¹⁰ T. Guo,⁵⁹ H. Guragain,¹⁸ T. Hachiya,^{53,54} J.S. Haggerty,⁷ K.I. Hahn,¹⁶ H. Hamagaki,¹⁰ H.F. Hamilton,¹ J. Hanks,⁵⁹ S.Y. Han,^{16,30} S. Hasegawa,²⁷ T.O.S. Haseler,¹⁸ T.K. Hemmick,⁵⁹ X. He,¹⁸ J.C. Hill,²⁶ K. Hill,¹¹ A. Hodges,^{18,23} R.S. Hollis,⁸ K. Homma,¹⁹ B. Hong,³⁰ T. Hoshino,¹⁹ N. Hotvedt,²⁶ J. Huang,⁷ K. Imai,²⁷ M. Inaba,⁶² A. Iordanova,⁸ D. Isenhower,¹ D. Ivanishchev,⁵² B. Jacak,⁵⁹ M. Jezghani,¹⁸ X. Jiang,³⁴ Z. Ji,⁵⁹ B.M. Johnson,^{7,18} D. Jouan,⁵⁰ D.S. Jumper,²³ J.H. Kang,⁶⁷ D. Kapukchyan,⁸ S. Karthas,⁵⁹ D. Kawall,³⁸ A.V. Kazantsev,³¹ V. Khachatryan,⁵⁹ A. Khanzadeev,⁵² C. Kim,^{8,30} E.-J. Kim,²⁸ M. Kim,⁵⁷ D. Kincses,¹⁵ E. Kistenev,⁷ J. Klatsky,¹⁷ P. Kline,⁵⁹ T. Koblesky,¹¹ D. Kotov,^{52,56} L. Kovacs,¹⁵ S. Kudo,⁶² K. Kurita,⁵⁵ Y. Kwon,⁶⁷ J.G. Lajoie,²⁶ A. Lebedev,²⁶ S. Lee,⁶⁷ M.J. Leitch,³⁴ Y.H. Leung,⁵⁹ S.H. Lim,^{34,67} M.X. Liu,³⁴ X. Li,³⁴ V.-R. Loggins,²³ S. Lökös,⁶⁶ D.A. Loomis,⁴⁰ K. Lovasz,¹⁴ D. Lynch,⁷ T. Majoros,¹⁴ Y.I. Makdisi,⁶ M. Makek,⁶⁸ V.I. Manko,³¹ E. Mannel,⁷ M. McCumber,³⁴ P.L. McGaughey,³⁴ D. McGlinchey,^{11,34} C. McKinney,²³ M. Mendoza,⁸ A.C. Mignerey,³⁷ A. Milov,⁶⁵ D.K. Mishra,⁴ J.T. Mitchell,⁷ M. Mitrnkova,^{56,59} Iu. Mitrnkov,^{56,59} G. Mitsuka,^{29,54} S. Miyasaka,^{53,61} S. Mizuno,^{53,62} P. Montuenga,²³ T. Moon,^{30,67} D.P. Morrison,⁷ B. Mulilo,^{30,53,69} T. Murakami,^{32,53} J. Murata,^{53,55} K. Nagai,⁶¹ K. Nagashima,¹⁹ T. Nagashima,⁵⁵ J.L. Nagle,¹¹ M.I. Nagy,¹⁵ I. Nakagawa,^{53,54} K. Nakano,^{53,61} C. Nattrass,⁶⁰ T. Niida,⁶² R. Nouicer,^{7,54} N. Novitzky,⁵⁹ T. Novák,^{39,66} G. Nukazuka,^{53,54} A.S. Nyanin,³¹ E. O'Brien,⁷ C.A. Ogilvie,²⁶ J.D. Orjuela Koop,¹¹ M. Orosz,^{14,21} J.D. Osborn,^{40,49} A. Oskarsson,³⁵ G.J. Ottino,⁴⁵ K. Ozawa,^{29,62} V. Pantuev,²⁴ V. Papavassiliou,⁴⁶ J.S. Park,⁵⁷ S. Park,^{41,53,57,59} M. Patel,²⁶ S.F. Pate,⁴⁶ D.V. Perepelitsa,^{7,11} G.D.N. Perera,⁴⁶ D.Yu. Peressounko,³¹ C.E. PerezLara,⁵⁹ J. Perry,²⁶ R. Petti,⁷ M. Phipps,^{7,23} C. Pinkenburg,⁷ R.P. Pisani,⁷ M. Potekhin,⁷ M.L. Purschke,⁷ K.F. Read,^{49,60} D. Reynolds,⁵⁸ V. Riabov,^{44,52} Y. Riabov,^{52,56} D. Richford,^{5,63} T. Rinn,²⁶ S.D. Rolnick,⁸ M. Rosati,²⁶ Z. Rowan,⁵ A.S. Safonov,⁵⁶ T. Sakaguchi,⁷ H. Sako,²⁷ V. Samsonov,^{44,52} M. Sarsour,¹⁸ S. Sato,²⁷ B. Schaefer,⁶⁴ B.K. Schmoll,⁶⁰ K. Sedgwick,⁸ R. Seidl,^{53,54} A. Seleznev,⁵⁶ A. Sen,^{26,60} R. Seto,⁸ A. Sexton,³⁷ D. Sharma,⁵⁹ I. Shein,²² T.-A. Shibata,^{53,61} K. Shigaki,¹⁹ M. Shimomura,^{26,43} T. Shioya,⁶² P. Shukla,⁴ A. Sickles,²³ C.L. Silva,³⁴ D. Silvermyr,³⁵ B.K. Singh,³ C.P. Singh,^{3,†} V. Singh,³ M. Slunečka,⁹ K.L. Smith,^{17,34} M. Snowball,³⁴ R.A. Soltz,³³ W.E. Sondheim,³⁴ S.P. Sorensen,⁶⁰ I.V. Sourikova,⁷ P.W. Stankus,⁴⁹ S.P. Stoll,⁷ T. Sugitate,¹⁹ A. Sukhanov,⁷ T. Sumita,⁵³ J. Sun,⁵⁹ Z. Sun,^{14,21,59} J. Sziklai,⁶⁶ K. Tanida,^{27,54,57} M.J. Tannenbaum,⁷ S. Tarafdar,^{64,65} G. Tarnai,¹⁴ R. Tieulent,^{18,36} A. Timilsina,²⁶ T. Todoroki,^{53,54,62} M. Tomášek,¹³ C.L. Towell,¹ R.S. Towell,¹ I. Tserruya,⁶⁵ Y. Ueda,¹⁹ B. Ujvari,^{14,21} H.W. van Hecke,³⁴ J. Velkovska,⁶⁴ M. Virius,¹³ V. Vrba,^{13,25} N. Vukman,⁶⁸ X.R. Wang,^{46,54} Y.S. Watanabe,¹⁰ C.L. Woody,⁷ L. Xue,¹⁸ C. Xu,⁴⁶ Q. Xu,⁶⁴ S. Yalcin,⁵⁹ Y.L. Yamaguchi,⁵⁹ H. Yamamoto,⁶² A. Yanovich,²² I. Yoon,⁵⁷ J.H. Yoo,³⁰ I.E. Yushmanov,³¹ H. Yu,^{46,51} W.A. Zajc,¹² A. Zelenski,⁶ and L. Zou⁸

(PHENIX Collaboration)

¹Abilene Christian University, Abilene, Texas 79699, USA

²Department of Physics, Augustana University, Sioux Falls, South Dakota 57197, USA

³Department of Physics, Banaras Hindu University, Varanasi 221005, India

⁴Bhabha Atomic Research Centre, Bombay 400 085, India

⁵Baruch College, City University of New York, New York, New York, 10010 USA

⁶Collider-Accelerator Department, Brookhaven National Laboratory, Upton, New York 11973-5000, USA

⁷Physics Department, Brookhaven National Laboratory, Upton, New York 11973-5000, USA

⁸University of California-Riverside, Riverside, California 92521, USA

⁹Charles University, Faculty of Mathematics and Physics, 180 00 Troja, Prague, Czech Republic

¹⁰Center for Nuclear Study, Graduate School of Science, University of Tokyo, 7-3-1 Hongo, Bunkyo, Tokyo 113-0033, Japan

¹¹University of Colorado, Boulder, Colorado 80309, USA

- ¹²Columbia University, New York, New York 10027 and Nevis Laboratories, Irvington, New York 10533, USA
- ¹³Czech Technical University, Zikova 4, 166 36 Prague 6, Czech Republic
- ¹⁴Debrecen University, H-4010 Debrecen, Egyetem tér 1, Hungary
- ¹⁵ELTE, Eötvös Loránd University, H-1117 Budapest, Pázmány P. s. 1/A, Hungary
- ¹⁶Ewha Womans University, Seoul 120-750, Korea
- ¹⁷Florida State University, Tallahassee, Florida 32306, USA
- ¹⁸Georgia State University, Atlanta, Georgia 30303, USA
- ¹⁹Physics Program and International Institute for Sustainability with Knotted Chiral Meta Matter (SKCM2), Hiroshima University, Higashi-Hiroshima, Hiroshima 739-8526, Japan
- ²⁰Department of Physics and Astronomy, Howard University, Washington, DC 20059, USA
- ²¹HUN-REN ATOMKI, H-4026 Debrecen, Bem tér 18/c, Hungary
- ²²IHEP Protvino, State Research Center of Russian Federation, Institute for High Energy Physics, Protvino, 142281, Russia
- ²³University of Illinois at Urbana-Champaign, Urbana, Illinois 61801, USA
- ²⁴Institute for Nuclear Research of the Russian Academy of Sciences, prospekt 60-letiya Oktyabrya 7a, Moscow 117312, Russia
- ²⁵Institute of Physics, Academy of Sciences of the Czech Republic, Na Slovance 2, 182 21 Prague 8, Czech Republic
- ²⁶Iowa State University, Ames, Iowa 50011, USA
- ²⁷Advanced Science Research Center, Japan Atomic Energy Agency, 2-4 Shirakata Shirane, Tokai-mura, Naka-gun, Ibaraki-ken 319-1195, Japan
- ²⁸Jeonbuk National University, Jeonju, 54896, Korea
- ²⁹KEK, High Energy Accelerator Research Organization, Tsukuba, Ibaraki 305-0801, Japan
- ³⁰Korea University, Seoul 02841, Korea
- ³¹National Research Center “Kurchatov Institute”, Moscow, 123098 Russia
- ³²Kyoto University, Kyoto 606-8502, Japan
- ³³Lawrence Livermore National Laboratory, Livermore, California 94550, USA
- ³⁴Los Alamos National Laboratory, Los Alamos, New Mexico 87545, USA
- ³⁵Department of Physics, Lund University, Box 118, SE-221 00 Lund, Sweden
- ³⁶IPNL, CNRS/IN2P3, Univ Lyon, Université Lyon 1, F-69622, Villeurbanne, France
- ³⁷University of Maryland, College Park, Maryland 20742, USA
- ³⁸Department of Physics, University of Massachusetts, Amherst, Massachusetts 01003-9337, USA
- ³⁹MATE, Institute of Technology, Laboratory of Femtoscopy, Károly Róbert Campus, H-3200 Gyöngyös, Mátrai út 36, Hungary
- ⁴⁰Department of Physics, University of Michigan, Ann Arbor, Michigan 48109-1040, USA
- ⁴¹Mississippi State University, Mississippi State, Mississippi 39762, USA
- ⁴²Muhlenberg College, Allentown, Pennsylvania 18104-5586, USA
- ⁴³Nara Women’s University, Kita-uoya Nishi-machi Nara 630-8506, Japan
- ⁴⁴National Research Nuclear University, MEPhI, Moscow Engineering Physics Institute, Moscow, 115409, Russia
- ⁴⁵University of New Mexico, Albuquerque, New Mexico 87131, USA
- ⁴⁶New Mexico State University, Las Cruces, New Mexico 88003, USA
- ⁴⁷Physics and Astronomy Department, University of North Carolina at Greensboro, Greensboro, North Carolina 27412, USA
- ⁴⁸Department of Physics and Astronomy, Ohio University, Athens, Ohio 45701, USA
- ⁴⁹Oak Ridge National Laboratory, Oak Ridge, Tennessee 37831, USA
- ⁵⁰IPN-Orsay, Univ. Paris-Sud, CNRS/IN2P3, Université Paris-Saclay, BP1, F-91406, Orsay, France
- ⁵¹Peking University, Beijing 100871, People’s Republic of China
- ⁵²PNPI, Petersburg Nuclear Physics Institute, Gatchina, Leningrad region, 188300, Russia
- ⁵³RIKEN Nishina Center for Accelerator-Based Science, Wako, Saitama 351-0198, Japan
- ⁵⁴RIKEN BNL Research Center, Brookhaven National Laboratory, Upton, New York 11973-5000, USA
- ⁵⁵Physics Department, Rikkyo University, 3-34-1 Nishi-Ikebukuro, Toshima, Tokyo 171-8501, Japan
- ⁵⁶Saint Petersburg State Polytechnic University, St. Petersburg, 195251 Russia
- ⁵⁷Department of Physics and Astronomy, Seoul National University, Seoul 151-742, Korea
- ⁵⁸Chemistry Department, Stony Brook University, SUNY, Stony Brook, New York 11794-3400, USA
- ⁵⁹Department of Physics and Astronomy, Stony Brook University, SUNY, Stony Brook, New York 11794-3800, USA
- ⁶⁰University of Tennessee, Knoxville, Tennessee 37996, USA
- ⁶¹Department of Physics, Tokyo Institute of Technology, Oh-okayama, Meguro, Tokyo 152-8551, Japan
- ⁶²Tomonaga Center for the History of the Universe, University of Tsukuba, Tsukuba, Ibaraki 305, Japan
- ⁶³United States Merchant Marine Academy, Kings Point, New York 11024, USA
- ⁶⁴Vanderbilt University, Nashville, Tennessee 37235, USA
- ⁶⁵Weizmann Institute, Rehovot 76100, Israel
- ⁶⁶Institute for Particle and Nuclear Physics, HUN-REN Wigner Research Centre for Physics, (HUN-REN Wigner RCP, RMI), H-1525 Budapest 114, POBox 49, Budapest, Hungary
- ⁶⁷Yonsei University, IPAP, Seoul 120-749, Korea
- ⁶⁸Department of Physics, Faculty of Science, University of Zagreb, Bijenička c. 32 HR-10002 Zagreb, Croatia
- ⁶⁹Department of Physics, School of Natural Sciences, University of Zambia, Great East Road Campus, Box 32379, Lusaka, Zambia

(Dated: September 6, 2024)

The J/ψ and $\psi(2S)$ charmonium states, composed of $c\bar{c}$ quark pairs and known since the 1970s, are widely believed to serve as ideal probes to test quantum chromodynamics in high-energy hadronic interactions. However, there is not yet a complete understanding of the charmonium-production mechanism. Recent measurements of J/ψ production as a function of event charged-particle multiplicity at the collision energies of both the Large Hadron Collider (LHC) and the Relativistic Heavy Ion Collider (RHIC) show enhanced J/ψ production yields with increasing multiplicity. One potential explanation for this type of dependence is multiparton interactions (MPI). We carry out the first measurements of self-normalized J/ψ yields and the $\psi(2S)$ to J/ψ ratio at both forward and backward rapidities as a function of self-normalized charged-particle multiplicity in $p+p$ collisions at $\sqrt{s} = 200$ GeV. In addition, detailed PYTHIA studies tuned to RHIC energies were performed to investigate the MPI impacts. We find that the PHENIX data at RHIC are consistent with recent LHC measurements and can only be described by PYTHIA calculations that include MPI effects. The forward and backward $\psi(2S)$ to J/ψ ratio, which serves as a unique and powerful approach to study final-state effects on charmonium production, is found to be less dependent on the charged-particle multiplicity.

Charmonium, a bound $c\bar{c}$ state, has been studied extensively over the past several decades, but a clear understanding of its formation has not yet been reached. Several models are currently available to describe the evolution of a $c\bar{c}$ pair into the bound J/ψ or $\psi(2S)$ meson, such as the nonrelativistic-quantum-chromodynamics (NRQCD) [1], color-evaporation [2], color-singlet [3], and jet-fragmentation [4] models. The formation appears to involve both perturbative (above the Λ_{QCD} scale) and nonperturbative (below the Λ_{QCD} scale) aspects of QCD. The initial creation of $c\bar{c}$ pairs through hard scattering can be described as perturbative, and their evolution into a color-neutral state is likely nonperturbative.

In this Letter, we present PHENIX measurements at the Relativistic Heavy Ion Collider (RHIC) of the self-normalized J/ψ production versus self-normalized event multiplicity to study the multi-parton-interaction (MPI) effects at forward rapidity as well as the $\psi(2S)$ to J/ψ ratio, which is sensitive to final-state interactions in $p+p$ collisions at RHIC energies. We measure inclusive J/ψ and $\psi(2S)$ production without separating prompt from nonprompt charmonium because the nonprompt contributions are less than 3% of the total charmonium production.

The STAR Experiment at RHIC has measured the self-normalized J/ψ yields as a function of self-normalized charged-particle multiplicity at midrapidity in $p+p$ collisions [5]. The results show an increase in the J/ψ yields with increasing multiplicity, a dependence suggesting MPI. Additionally, at Large-Hadron-Collider (LHC) energies, the ALICE experiment has reported similar results for the normalized J/ψ yields versus event multiplicity at both forward rapidity [6, 7] and midrapidity [8]. In addition to potential MPI, the $\psi(2S)$ to J/ψ ratio could reveal final-state effects from either hot (formation of quark-gluon plasma [9–12]), or cold (comover-interaction model [13]) nuclear-matter effects. In early 2024, the

LHCb collaboration reported the ratio of the normalized $\psi(2S)$ to J/ψ in $p+p$ collisions at $\sqrt{s} = 13$ TeV as a function of multiplicity [14], where suppression of promptly produced charmonia is observed at high event multiplicity.

The present analysis relies on the data from the PHENIX experiment [15] obtained using the muon-arms detector subsystem covering $1.2 < |\eta| < 2.4$, which includes the muon tracker (MuTr), the muon identifier (MuID), the hadron absorbers, the forward silicon vertex detectors (FVTX) [16–19] in the forward rapidity region and the central arm barrel silicon vertex tracker (VTX) [20] at $|\eta| < 1.0$. Two beam-beam counters (BBC), covering the full azimuth and $3.1 < |\eta| < 3.9$, measure the vertex position along the beamline, located at $z = \pm 144$ cm from the nominal interaction point. The BBCs also serve as the minimum-bias (MB) trigger and measure the beam luminosity.

The $p+p$ data set used in this analysis was collected in 2015 and recorded at $\sqrt{s} = 200$ GeV center-of-mass energy. The analyzed events were selected by the MB trigger and the dimuon triggers, which required two or more muon tracks in the MuID. The collision vertex was constrained to be within ± 10 cm with respect to the center of the interaction region. The total sampled luminosity for the $p+p$ data set is 47 pb^{-1} .

The observable used in this analysis has theoretical [21] and experimental [22] motivations. We first define the self-normalized event charged-particle multiplicity $N_{\text{ch}}/\langle N_{\text{ch}} \rangle$, where N_{ch} represents the number of reconstructed charged-particle tracks detected by the forward- or backward-rapidity FVTX with $1.2 < \eta < 2.4$ and $-2.4 < \eta < -1.2$, and $\langle N_{\text{ch}} \rangle$ represents the average N_{ch} for MB events. Then the relative yield of J/ψ , denoted as $N_{J/\psi}/\langle N_{J/\psi} \rangle$ in a given $N_{\text{ch}}/\langle N_{\text{ch}} \rangle$ range, is measured by the forward or backward muon arms covering $1.2 < y < 2.2$ and $-2.2 < y < -1.2$, respectively:

$$N_{J/\psi}/\langle N_{J/\psi} \rangle = \frac{N_{J/\psi}^{\text{raw}}}{N_{\text{evt}}} \frac{N_{\text{evt}}^{\text{total}}}{N_{J/\psi}^{\text{raw, total}}} \frac{\varepsilon_{\text{trig}}^{\text{MB}}}{\varepsilon_{\text{trig}}} \frac{\langle \varepsilon_{\text{trig}}^{J/\psi} \rangle}{\langle \varepsilon_{\text{trig}}^{\text{MB}} \rangle} f_{\text{coll}}, \quad (1)$$

where $N_{J/\psi}^{\text{raw}}$ is the raw number of J/ψ signal yield ex-

* PHENIX Spokesperson: akiba@rcf.rhic.bnl.gov

† Deceased

tracted from the dimuon invariant mass fit, and N_{evt} is the number of recorded MB events for a certain N_{ch} bin. The average MB efficiency is $\langle \epsilon_{\text{trig}}^{\text{MB}} \rangle = 55 \pm 5\%$ and the J/ψ efficiency is $\langle \epsilon_{\text{trig}}^{J/\psi} \rangle = 79 \pm 2\%$. The superscript “total” stands for quantities integrated over all N_{ch} . The $\epsilon_{\text{trig}}^{\text{MB}}$ is the MB trigger efficiency, $\epsilon_{\text{trig}}^{J/\psi}$ is the dimuon trigger efficiency. The f_{coll} is a correction factor for multiple collisions. The same observable is then measured for $\psi(2S)$, and the ratio of relative yields is defined as $(N_{\psi(2S)}/N_{J/\psi})/\langle N_{\psi(2S)}/N_{J/\psi} \rangle$. We present the data in terms of the same arms defined as measuring N_{ch} and $N_{J/\psi}$ at the same rapidity range, and opposite arms defined as measuring N_{ch} and $N_{J/\psi}$ at the opposite rapidity range. When combining the data from two arms, we define $1.2 < |\eta| < 2.4$ for N_{ch} and $1.2 < |y| < 2.2$ for $N_{J/\psi}$.

In PHENIX the trigger efficiency has event-multiplicity dependence due to finite acceptance of the BBC. The event multiplicity-dependent MB and dimuon trigger efficiencies are determined using a data-driven approach. The MB trigger efficiency versus event multiplicity was evaluated with random-collision-clock triggered events by checking whether the MB trigger is fired for events satisfying the MB trigger condition. To check the multiplicity dependence of the MB trigger for hard-scattering events, we require at least one EMCAL cluster of $E > 2$ GeV on top of the random-collision-clock trigger

The possibility of multiple-collision events, defined as an event having $p+p$ collisions in addition to the one that produced the J/ψ or $\psi(2S)$, increases with increasing multiplicity. A data-driven method is utilized to estimate the fraction of multiple collision events, which assumes Poisson statistics and estimates the BBC (MB) trigger rate R_{BBC} using the following formula:

$$R_{\text{BBC}} = f_{\text{BC}}[1 - e^{-\mu\epsilon_F} - e^{-\mu\epsilon_B} - e^{-\mu(\epsilon_F + \epsilon_B + \epsilon_{FB})}], \quad (2)$$

where f_{BC} is the beam-crossing rate at RHIC, μ is the mean number of collisions, ϵ_F (ϵ_B) is the trigger efficiency ($\approx 75\%$) of each BBC at forward (backward) rapidity, and ϵ_{FB} is the trigger efficiency ($\approx 50\%$) when both BBCs are fired. The maximum R_{BBC} during the $p+p$ data run is 2.5 MHz, corresponding to an $\approx 10\%$ rate of double collision events. Due to the average R_{BBC} being ≈ 1 MHz and the low probability of having more than two collisions per beam crossing, only contributions from double collisions were considered. The ratio of double to single collisions, f_{coll} , is evaluated as a function of the measured-BBC-trigger rate R_{BBC} .

A crystal-ball (CB) function [24] is used to model the J/ψ and $\psi(2S)$ signal shapes to extract the raw yields from the dimuon invariant-mass distribution. The tail parameters α and n of the CB function were fixed with values from integrated multiplicity data for J/ψ and simulation studies for $\psi(2S)$. The FVTX detector delivers the mass resolution needed for $\psi(2S)$ measurements but reduces the acceptance due to a finite matching efficiency between the MuTr and FVTX detectors.

For $N_{J/\psi}/\langle N_{J/\psi} \rangle$ as a function of $N_{\text{ch}}/\langle N_{\text{ch}} \rangle$ shown in Figs. 1 and 2, the FVTX detector is not used to maximize J/ψ signal statistics. For $\psi(2S)$ measurements with the FVTX detector, a Gaussian function is used alongside the CB function to account for the broadening of signal shape due to misassociation between the FVTX and MuTr detectors [25]. The individual multiplicity bins are fitted by fixing the shape parameters of the CB function to the integrated multiplicity fit results to extract the J/ψ signal yield.

For the J/ψ analysis without the FVTX detector, an exponential decay function is used to describe the background. For the $\psi(2S)$ to J/ψ ratio, a modified Hagedorn function is used to model the combinatorial and correlated-background contributions [26, 27]. The shape of the combinatorial background is estimated with real data using the mixed-event method, where opposite sign single muons are selected from different events. The combinatorial background normalization is obtained from like-sign single muons selected from the same events. The correlated background shape is determined using detailed simulation studies [26] and is implemented in the total fit function by fixing three of the five parameters of the modified Hagedorn function to constrain the shape.

The sources of systematic uncertainties for the J/ψ measurements include the following: the J/ψ reconstruction efficiency, the J/ψ trigger efficiency, the MB trigger efficiency, and the multiple-collision-correction factor f_{coll} per beam crossing. A systematic uncertainty is assigned for the J/ψ reconstruction efficiency based on the largest variation when three different z -vertex selections are applied. For the systematic uncertainty related to the J/ψ trigger efficiency, the efficiency as a function of N_{ch} is first fit with the following function: $f(x) = p_0 + p_1 e^{-p_2 x}$. Then, the efficiency distribution is re-evaluated by moving the parameter values by $\pm 1\sigma$ of the statistical uncertainty in the fit result. The largest difference with respect to the nominal value is assigned as the systematic uncertainty. The MB-trigger efficiency can be affected by multiple collisions. The systematic uncertainty related to the MB-trigger efficiency is determined by dividing the trigger efficiency into three different $p+p$ collision rates, determined by the MB trigger: 600–800, 1000–1500, and 2000–2500 kHz. The trigger efficiency for the high and low trigger rates are compared to the central rate, and the maximum deviation is scaled by $1/\sqrt{12}$ (the standard deviation of a uniform distribution), which is assigned as the systematic uncertainty. The systematic uncertainty related to the multiple-collision correction factor is evaluated by comparing correction factors using an alternate method, which is the ratio of probability distributions $P(N_{\text{ch}})$ between two different trigger rates, less than 500 and 1000–1500 kHz.

The sources of systematic uncertainty for the normalized $\psi(2S)$ to J/ψ ratio include the following: the mixed-event background normalization, the signal shapes (fixed CB tail parameters and the second Gaussian width), and the correlated background shape. Most systematic un-

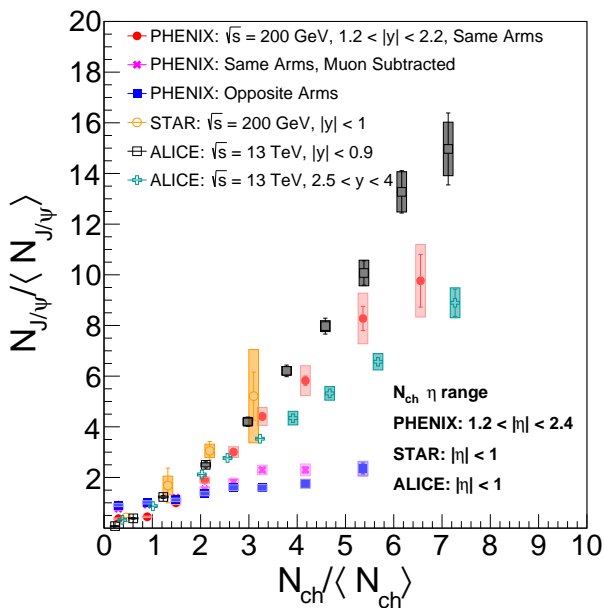


FIG. 1. The self-normalized J/ψ yield as a function of self-normalized charged-particle multiplicity in $p+p$ collisions at various energies. The PHENIX data combine forward and backward J/ψ with forward and backward FVTX, respectively. The contribution of J/ψ daughter-muon tracks included in the charged-particle multiplicity (solid circle) and the ones subtracting the J/ψ daughter-muon-tracks contribution (solid cross) in the same arms as well as the ones with opposite arm (solid square) are presented. The PHENIX measurements are compared with ALICE measurements at forward rapidity [7] and at midrapidity [8], and STAR [5] measurements at midrapidity. The error bars (boxes) denote the statistical (systematic) uncertainties.

certainties cancel for the double ratio, including uncertainties related to fixing the CB tail parameters, the second Gaussian width, and the multiple collision correction factor. The correlated background uncertainty was determined by allowing two of the five parameters in the fit function to vary and comparing the resulting signal yields from each fit. The determination of the uncertainty in the normalization of the mixed-event background follows the methods described in Ref. [25] and an uncertainty is assigned by repeating the fit to the invariant-mass distribution over a mass range extended first below and then above the nominal mass range of the fit.

The self-normalized J/ψ yields ($N_{J/\psi}/\langle N_{J/\psi} \rangle$) as a function of self-normalized charged-particle multiplicity ($N_{ch}/\langle N_{ch} \rangle$) are shown in Fig. 1 and compared to STAR [5] and ALICE [7, 8] data. The J/ψ decay-daughter-muon contributions to the charged-particle multiplicity have been subtracted in the PHENIX results to remove the auto-correlation effect. Before subtracting the J/ψ daughter-muon contributions, The PHENIX results show a multiplicity dependence that is similar

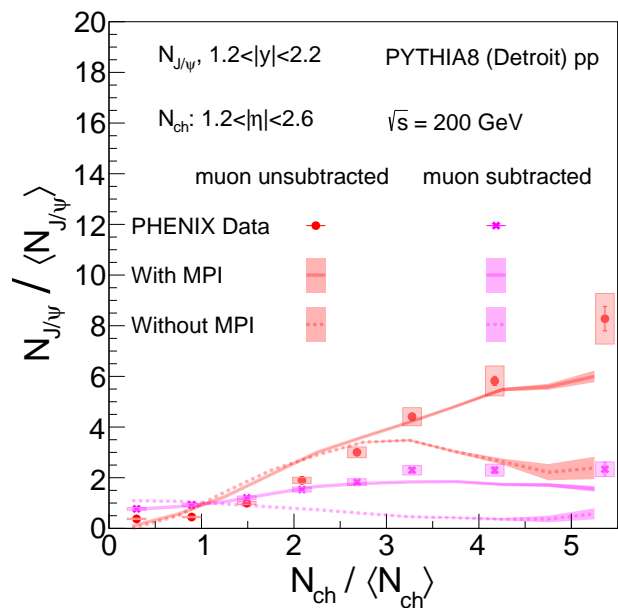


FIG. 2. The self-normalized J/ψ yields are shown as a function of self-normalized charged-particle multiplicity in $p+p$ collisions at $\sqrt{s} = 200$ GeV. The solid circle and solid cross data points, respectively, represent the measurements before and after the J/ψ muon tracks have been subtracted (see text for more details). The error bars (boxes) denote the statistical (systematic) uncertainties. Data are compared to PYTHIA8 Detroit tuned calculations in the pseudorapidity range of $2.1 < |\eta| < 2.6$ for charged particles with (solid lines) and without (dash lines) considering MPI effects [23].

to the STAR results at midrapidity. For ALICE at 13 TeV, the results at forward rapidity are systematically lower than at midrapidity, but it is difficult to reach conclusions for PHENIX and STAR at 200 GeV due to the larger systematic uncertainties. After subtracting the J/ψ daughter-muon contributions, the J/ψ yields shift to lower $N_{ch}/\langle N_{ch} \rangle$, leading to a significant drop of $N_{J/\psi}/\langle N_{J/\psi} \rangle$, which is consistent with the results of opposite arms, where N_{ch} is free from the J/ψ daughter-muon contributions. The PHENIX results with subtraction is significantly lower than the ALICE results at forward rapidity, but a comparable slope is seen in STAR and ALICE results at midrapidity. Note that the auto-correlation correction was not applied to the ALICE and STAR results. The impact on the slope is expected to be more significant for the STAR than the ALICE results due to the smaller multiplicity.

The self-normalized J/ψ yields are also compared with PYTHIA8 calculations. In Fig. 2 where the simulations are compared to J/ψ normalized yield in data, the PYTHIA8 Detroit tuned with MPI calculations [29] agree with the

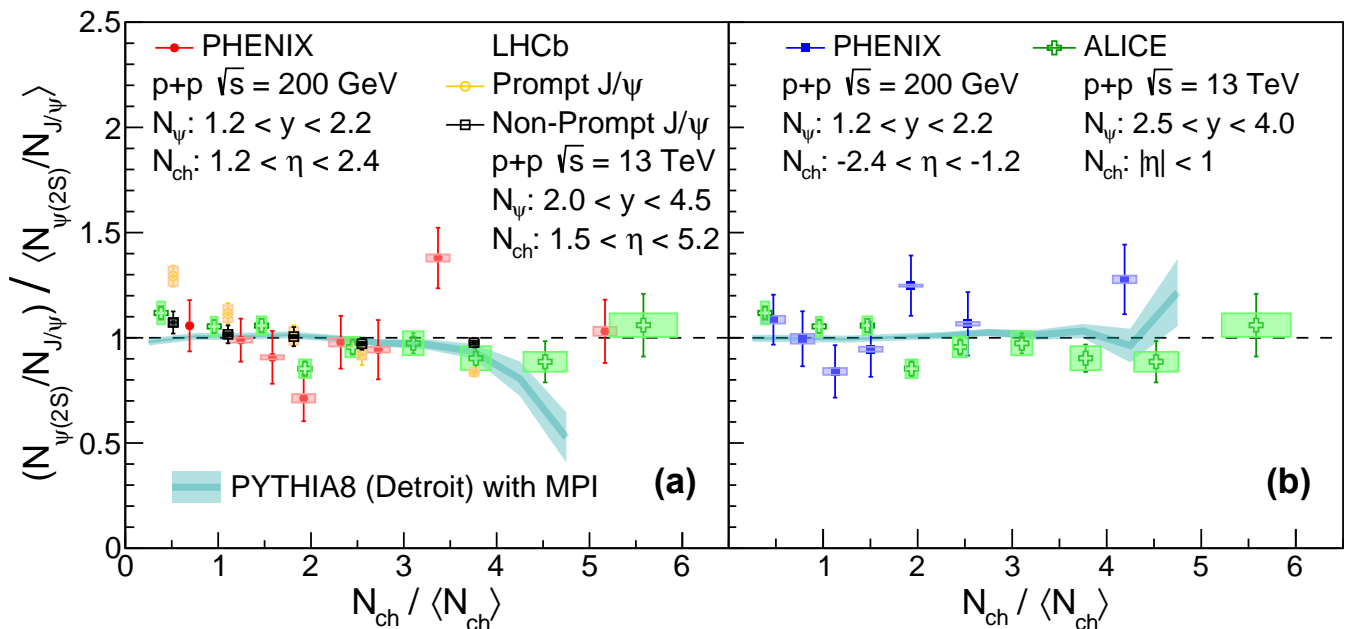


FIG. 3. The self-normalized $\psi(2S)$ to J/ψ ratio at forward rapidity as a function of self-normalized charged-particle multiplicity in $p+p$ collisions at $\sqrt{s} = 200$ GeV by PHENIX compared with the (a) LHCb and (b) ALICE results at $\sqrt{s} = 13$ TeV [28]. The PHENIX data is compared when charged particles are measured at (a) forward rapidity and (b) backward rapidity. In addition, the data are compared to Detroit tuned [29] ([cyan] curve), including MPI effects. The error bars (boxes) denote the statistical (systematic) uncertainties.

data within $\approx 1\sigma$ while failing to describe the data without MPI effects. Therefore, MPI effects need to be included to accurately model J/ψ production in $p+p$ collisions at RHIC. In addition, comparison between the PHENIX and ALICE results at forward rapidity indicates that the MPI effects on the multiplicity dependence would be even stronger at LHC energies.

The $(N_{\psi(2S)}/N_{J/\psi})/\langle N_{\psi(2S)}/N_{J/\psi} \rangle$ as a function of $N_{ch}/\langle N_{ch} \rangle$, shown in Fig. 3, was measured to investigate final-state interaction effects on charmonium production. The self-normalized yield ratios of $\psi(2S)$ to J/ψ at forward rapidity are shown as a function of normalized charged-particle multiplicity, where the charged-particle multiplicity has been measured using both the forward (same arms) and backward (opposite arms) FVTX detectors. The $(N_{\psi(2S)}/N_{J/\psi})/\langle N_{\psi(2S)}/N_{J/\psi} \rangle$ measurements are consistent with unity within $\approx 1\sigma$, and no significant rapidity dependence is observed. Therefore, final-state interactions on charmonium production appear negligible at the measured multiplicity range and collision energy.

Furthermore, in Fig. 3, the ALICE forward rapidity prompt J/ψ [28] and LHCb prompt and nonprompt J/ψ measurements are included for comparison. The ALICE results also demonstrate similar consistency near unity up to $N_{ch}/\langle N_{ch} \rangle \approx 6$. Recently, LHCb has reported suppression of $(N_{\psi(1S)}/N_{J/\psi})/\langle N_{\psi(1S)}/N_{J/\psi} \rangle$ in high multiplicity $p+p$ collisions [14]. The final state comover effect [13] becomes more pronounced at high multiplicity, and may result in the increased breakup of $\psi(2S)$ compared to J/ψ due to its lower binding energy.

Finally, Fig. 3 also shows PYTHIA8 Detroit tuned with MPI effects for the $(N_{\psi(2S)}/N_{J/\psi})/\langle N_{\psi(2S)}/N_{J/\psi} \rangle$ as a function of $N_{ch}/\langle N_{ch} \rangle$ but without any final-state effects on quarkonia. The PYTHIA8 calculations yield similar results within uncertainties, and generally reproduce the data near unity. This indicates that the data favors no significant final-state interaction in $p+p$ collisions at $\sqrt{s} = 200$ GeV.

In summary, we have reported multiplicity-dependent studies of J/ψ and $\psi(2S)$ production at forward rapidity in $p+p$ collisions at $\sqrt{s} = 200$ GeV. The self-normalized J/ψ yields are measured up to ≈ 6 units of $N_{ch}/\langle N_{ch} \rangle$ and reasonable consistency with the STAR and ALICE data has been achieved when the J/ψ and charged particles are measured in the same pseudorapidity region. Results of self-normalized J/ψ yields before and after J/ψ decay-daughter-muon subtraction for N_{ch} counting can be well described by the PYTHIA8 Detroit tuned with MPI. Also, forward self-normalized $\psi(2S)$ to J/ψ yields as a function of forward and backward track multiplicity have been studied. Agreements with unity have been observed within uncertainties and the results are consistent with each other at different rapidity gaps, suggesting no significant final-state interactions on charmonium production. The PYTHIA8 model without final-state interactions generally reproduces the self-normalized $\psi(2S)$ to J/ψ yields indicating that no such effect occurs in $p+p$ collisions at RHIC energies.

Consistency with unity is also reported by ALICE. However, LHCb observes a suppression of prompt $\psi(2S)$

production at high multiplicity, aligning with the prediction of final-state comover effects [30]. The LHCb results also demonstrate consistency with the PHENIX data points within uncertainties. Investigations of charmonium production in p +Al and p +Au collisions with PHENIX data, particularly in the backward-rapidity region, would provide an excellent opportunity to further study final-state effects in small collision systems at RHIC energies.

We thank the staff of the Collider-Accelerator and Physics Departments at Brookhaven National Laboratory and the staff of the other PHENIX participating institutions for their vital contributions. We acknowledge support from the Office of Nuclear Physics in the Office of Science of the Department of Energy, the National Science Foundation, Abilene Christian University Research Council, Research Foundation of SUNY, and Dean of the College of Arts and Sciences, Vanderbilt University (U.S.A), Ministry of Education, Culture, Sports, Science, and Technology and the Japan Society for the Promotion of Science (Japan), Conselho Nacional de Desenvolvimento Científico e Tecnológico and Fundação de Amparo à Pesquisa do Estado de São Paulo (Brazil),

Natural Science Foundation of China (People's Republic of China), Croatian Science Foundation and Ministry of Science and Education (Croatia), Ministry of Education, Youth and Sports (Czech Republic), Centre National de la Recherche Scientifique, Commissariat à l'Énergie Atomique, and Institut National de Physique Nucléaire et de Physique des Particules (France), J. Bolyai Research Scholarship, EFOP, HUN-REN ATOMKI, NKFIH, MATE KKF, and OTKA (Hungary), Department of Atomic Energy and Department of Science and Technology (India), Israel Science Foundation (Israel), Basic Science Research and SRC(CENuM) Programs through NRF funded by the Ministry of Education and the Ministry of Science and ICT (Korea). Ministry of Education and Science, Russian Academy of Sciences, Federal Agency of Atomic Energy (Russia), VR and Wallenberg Foundation (Sweden), University of Zambia, the Government of the Republic of Zambia (Zambia), the U.S. Civilian Research and Development Foundation for the Independent States of the Former Soviet Union, the Hungarian American Enterprise Scholarship Fund, the US-Hungarian Fulbright Foundation, and the US-Israel Binational Science Foundation.

-
- [1] N. Brambilla, A. Pineda, J. Soto, and A. Vairo, Potential NRQCD: An Effective theory for heavy quarkonium, *Nucl. Phys. B* **566**, 275 (2000).
- [2] J. F. Amundson, O. J. P. Eboli, E. M. Gregores, and F. Halzen, Quantitative tests of color evaporation: Charmonium production, *Phys. Lett. B* **390**, 323 (1997).
- [3] J. H. Kuhn, S. Nussinov, and R. Ruckl, Charmonium Production in B Decays, *Z. Phys. C* **5**, 117 (1980).
- [4] M. Baumgart, A. K. Leibovich, T. Mehen, and I. Z. Rothstein, Probing Quarkonium Production Mechanisms with Jet Substructure, *J. High Energy Phys.* **11** (2014), 003.
- [5] J. Adam *et al.* (STAR Collaboration), J/ψ production cross section and its dependence on charged-particle multiplicity in $p+p$ collisions at $\sqrt{s} = 200$ GeV, *Phys. Lett. B* **786**, 87 (2018).
- [6] B. Abelev *et al.* (ALICE Collaboration), J/ψ polarization in pp collisions at $\sqrt{s} = 7$ TeV, *Phys. Rev. Lett.* **108**, 082001 (2012).
- [7] S. Acharya *et al.* (ALICE Collaboration), Forward rapidity J/ψ production as a function of charged-particle multiplicity in pp collisions at $\sqrt{s} = 5.02$ and 13 TeV, *J. High Energy Phys.* **06** (2022), 015.
- [8] S. Acharya *et al.* (ALICE Collaboration), Multiplicity dependence of J/ψ production at midrapidity in pp collisions at $\sqrt{s} = 13$ TeV, *Phys. Lett. B* **810**, 135758 (2020).
- [9] I. Arsene *et al.* (BRAHMS Collaboration), Quark gluon plasma and color glass condensate at RHIC? The Perspective from the BRAHMS experiment, *Nucl. Phys. A* **757**, 1 (2005).
- [10] K. Adcox *et al.* (PHENIX Collaboration), Formation of dense partonic matter in relativistic nucleus-nucleus collisions at RHIC: Experimental evaluation by the PHENIX collaboration, *Nucl. Phys. A* **757**, 184 (2005).
- [11] B. B. Back *et al.* (PHOBOS Collaboration), The PHOBOS perspective on discoveries at RHIC, *Nucl. Phys. A* **757**, 28 (2005).
- [12] J. Adams *et al.* (STAR Collaboration), Experimental and theoretical challenges in the search for the quark gluon plasma: The STAR Collaboration's critical assessment of the evidence from RHIC collisions, *Nucl. Phys. A* **757**, 102 (2005).
- [13] E. G. Ferreira, Excited charmonium suppression in proton-nucleus collisions as a consequence of comovers, *Phys. Lett. B* **749**, 98 (2015).
- [14] R. Aaij *et al.* (LHCb Collaboration), Multiplicity dependence of $\sigma_{(2S)}/\sigma_{J/\psi}$ in pp collisions at $\sqrt{s} = 13$ TeV, *J. High Energy Phys.* **05** (2024), 243.
- [15] D. P. Morrison *et al.* (PHENIX Collaboration), The PHENIX experiment at RHIC, *Nucl. Phys. A* **638**, 565 (1998).
- [16] H. Akikawa *et al.* (PHENIX Collaboration), PHENIX muon arms, *Nucl. Instrum. Methods Phys. Res., Sec. A* **499**, 537 (2003).
- [17] S. Adachi *et al.*, Trigger electronics upgrade of PHENIX muon tracker, *Nucl. Instrum. Methods Phys. Res., Sec. A* **703**, 114 (2013).
- [18] C. Aidala *et al.*, The PHENIX Forward Silicon Vertex Detector, *Nucl. Instrum. Methods Phys. Res., Sec. A* **755**, 44 (2014).
- [19] M. Allen *et al.* (PHENIX Collaboration), PHENIX inner detectors, *Nucl. Instrum. Methods Phys. Res., Sec. A* **499**, 549 (2003).
- [20] R. Nouicer (PHENIX Collaboration), PHENIX Upgrade: Novel Stripixel Detector for Heavy Quark Detection and Proton Spin Structure Measurements at RHIC Energies, *Nucl. Instrum. Methods Phys. Res., Sec. A* **261**, 1067 (2007).
- [21] E. G. Ferreira and C. Pajares, High multiplicity pp events

- and J/ψ production at energies available at the CERN Large Hadron Collider, Phys. Rev. C **86**, 034903 (2012).
- [22] B. Abelev *et al.* (ALICE Collaboration), J/ψ production as a function of charged particle multiplicity in pp collisions at $\sqrt{s}=7$ TeV, Phys. Lett. B **712**, 165 (2012).
- [23] J. Oh and S. Lim, Simulation study of multiplicity-dependent charmonia production with PYTHIA, J. Korean Phys. Soc. **82**, 651 (2023).
- [24] J. E. Gaiser, *Charmonium Spectroscopy From Radiative Decays of the J/ψ and ψ'* , Masters thesis, Stanford University (1982), SLAC-0255, UMI-83-14449-MC, SLAC-R-0255, SLAC-R-255.
- [25] A. Adare *et al.* (PHENIX Collaboration), Measurement of the relative yields of $\psi(2S)$ to $\psi(1S)$ mesons produced at forward and backward rapidity in $p+p$, $p+Al$, $p+Au$, and ^3He+Au collisions at $\sqrt{s_{NN}}=200$ GeV, Phys. Rev. C **95**, 034904 (2017).
- [26] C. Aidala *et al.* (PHENIX Collaboration), Measurements of $\mu\mu$ pairs from open heavy flavor and Drell-Yan in $p+p$ collisions at $\sqrt{s} = 200$ GeV, Phys. Rev. D **99**, 072003 (2019).
- [27] U. A. Acharya *et al.* (PHENIX Collaboration), Measurement of $\psi(2S)$ nuclear modification at backward and forward rapidity in $p+p$, $p+Al$, and $p+Au$ collisions at $\sqrt{s_{NN}} = 200$ GeV, Phys. Rev. C **105**, 064912 (2022).
- [28] S. Acharya *et al.* (ALICE Collaboration), Measurement of $\psi(2S)$ production as a function of charged-particle pseudorapidity density in pp collisions at $\sqrt{s} = 13$ TeV and p-Pb collisions at $\sqrt{s_{NN}} = 8.16$ TeV with ALICE at the LHC, J. High Energy Phys. **06** (2023), 147.
- [29] M. R. Aguilar, Z. Chang, R. K. Elayavalli, R. Fatemi, Y. He, Y. Ji, D. Kalinkin, M. Kelsey, I. Mooney, and V. Verkest, PYTHIA8 underlying event tune for RHIC energies, Phys. Rev. D **105**, 016011 (2022).
- [30] E. Ferreiro, Charmonium dissociation and recombination at LHC: Revisiting comovers, Phys. Lett. B **731**, 57 (2014).